Thermal stress analysis in a functionally graded hollow elliptic-cylinder subjected to uniform temperature distribution

V. R. Manthena
RTM Nagpur University

N. K. Lamba
Shri Lemdeo Patil Mahavidyalaya

G. D. Kedar
RTM Nagpur University

Thermal stress analysis in a functionally graded hollow elliptic-cylinder subjected to uniform temperature distribution

V. R. Manthena[a], N. K. Lamba[b], G. D. Kedar[a]

[a]Department of Mathematics
RTM Nagpur University
Nagpur, India

[b]Department of Mathematics
Shri Lemdeo Patil Mahavidyalaya
Nagpur, India
vkmanthena@gmail.com

Abstract

In this paper, an analytical method of a thermoelastic problem for a medium with functionally graded material properties is developed in a theoretical manner for the elliptic-cylindrical coordinate system under the assumption that the material properties except for Poisson's ratio and density are assumed to vary arbitrarily with the exponential law in the radial direction. An attempt has been made to reconsider the fundamental system of equations for functionally graded solids in a two-dimensional state under thermal and mechanical loads. The general solution of displacement formulation is obtained by the introduction of appropriate transformation and carried out the analysis by taking into account the variation of inhomogeneity parameters. Furthermore, the aforementioned problem degenerated into the problem of the circular region by applying limiting conditions, and the results are validated. Numerical computations are carried out for ceramic-metal-based functionally graded material, in which zirconia is selected as ceramic and aluminium as metal and are represented graphically.

1. Introduction

In the present day of designing applications, curved structures are being utilized widely due to the integrated advantage of amalgamating physical, mechanical, as well as thermal properties of various materials compared to objects of other shapes. Many of these applications require a

613

complete cognizance of transient temperature and heat flux distribution within the elliptical profiles. Things get further complicated and unpredictable once sectional heat supply is impacted on the object under consideration. Both analytical and numerical techniques are the most used methods to unravel such issues. Nonetheless, numerical solutions are preferred and prevalent in practice, due to either unavailability or higher mathematical complexity of the corresponding exact solutions. Exact solutions find their applications in validating and comparing various numerical algorithms to help improve the computational efficiency of computer codes that currently rely on numerical techniques. Although heat conduction problems for elliptical profile shape have been studied in great detail and various solution methods have been arrived at, one notable exception is an elliptical nuclear fuel rod, which is a new type of nuclear fuel rod included in nuclear reactors.

One-dimensional calculation of thermal residual stresses, arising from the fabrication of a functionally graded material (FGM) and pressurized thick-walled hollow circular cylinder are studied by Ravichandran (1995) and Nejad and Rahimi (2009). Zimmerman and Lutz (1999) derived the exact solution for the problem of uniformly heating cylinder whose elastic moduli and thermal expansion coefficient vary linearly with radius and found that the effective thermal expansion coefficient is essentially given by the volumetric average of the local thermal expansion coefficient, with the variation in moduli having only a small effect. Chen et al. (2001, 2002) studied the axisymmetric thermoelastic problem of a functionally graded transversely isotropic cylindrical shell and hollow cylinder due to uniform heat supply. Ootao and Tanigawa (2005) presented the theoretical treatment of transient thermoelastic problem involving a functionally graded hollow cylinder due to uniform heat supply by expressing the thermal and thermoelastic constants of the hollow cylinder as power functions of the radial coordinate. Noda et al. (2012) studied the theoretical treatment of a transient thermoelastic problem involving a functionally graded solid circular disk with piecewise power law due to uniform heat supply from an outer surface. The thermal conductivity, Young's modulus and the coefficient of linear thermal expansion of each layer, except the first inner layer, are expressed as power functions of the radial coordinate.

Tutuncu (2007) obtained the power series solutions for stresses and displacements in functionally graded cylindrical vessels subjected to internal pressure alone using the infinitesimal theory of elasticity by assuming the material to be isotropic with constant Poisson's ratio and exponentially-varying elastic modulus through the thickness. Abrinia et al. (2008) presented an analytical solution for computing the radial and circumferential stresses in an FGM thick cylindrical vessel under the influence of internal pressure and temperature is presented in this paper. Foroutan et al. (2011) carried out static analysis of FGM cylinders subjected to internal and external pressure by a mesh-free method by assuming the mechanical properties to vary in the radial direction. Ghannad and Gharooni (2012) presented displacements and stresses based on the high-order shear deformation theory (HSDT) for axisymmetric thick- walled cylinders made of functionally graded materials under internal and/or external uniform pressure, using the infinitesimal theory of elasticity and analytical formulation. Nejad et al. (2012) derived exact closed-form solutions for stresses and the displacements in thick spherical shells made of functionally graded materials with exponential-varying properties subjected to internal and external pressure. Ghannad and Gharooni (2013) obtained displacements and stresses in a rotating functionally graded pressurized thick-walled hollow circular cylindrical shell based on the first-order shear deformation theory (FSDT), using the infinitesimal theory of elasticity and analytical formulation. The material properties are

Manthena et al.: Thermal stress analysis in a functionally graded hollow elliptic

AAM: Intern. J., Vol 12, Issue 1 (June 2017)   615

assumed to be isotropic heterogeneous with constant Poisson's ratio and radially exponentially varying modulus of elasticity and density. Kursun et al. (2014) studied thermal elastic stress distribution occurred on long hollow cylinders made of FGM under thermal, mechanical and thermomechanical loads. Takabi (2016) presented an analytical and a numerical thermomechanical investigation of a thick walled cylinder made of the FGMs subjected to a pressure and a thermal load, and the properties of this material are varying across the thickness from the inner face that is a ceramic to the outer one which is a metal.

Topal and Gulgec (2009) considered the plane strain problem for a functionally graded solid cylinder with thermal energy generation under the effect of convective heat transfer and determined the thermal stresses. Hosseini and Akhlaghi (2009) studied transient thermal stresses in a thick hollow cylinder made of an FGM by considering the material properties to be nonlinear with a power law distribution through the thickness, and the cylinder is assumed to be of infinite length. Khorshidvand et al. (2010, 2012) presented a new solution for one-dimensional steady-state mechanical and thermal stresses in an FG rotating thick hollow cylinder by assuming the temperature distribution to be a function of radius along the thickness, with general thermal and mechanical boundary conditions on surfaces of the cylinder.

From the above literature review, it is observed that several kinds of boundary value problems in an axisymmetrical or one-dimensional state have been studied. However, it is obviously seen that the fundamental equation system proposed is not sufficient to solve thermoelastic boundary value problems under thermal and mechanical loads satisfying all the mechanical boundary conditions. To fill this gap, the two arbitrary constants from the second order differential equation are obtained using mechanical boundary conditions for two-dimensional axisymmetrical problem.

In the present paper, we have considered a two-dimensional transient thermoelastic problem of an elliptic-cylinder occupying the space $a \le \xi \le b$, $0 \le z \le \ell$, subjected to uniform temperature distribution. For theoretical treatment, all physical and mechanical quantities are taken as dimensional, whereas for numerical computations we have considered non-dimensional parameters.

2. Formulation of the problem

2.1. Statement of governing equations

We consider a functionally graded hollow elliptic-cylinder with thickness ℓ, internal radius a and external radius b, occupying the space

$$D = \{(\xi, z) \in R^2 : a < \xi < b, \, 0 \le z \le \ell\};$$

defined by the transformation

$$\xi + i\eta = \cosh^{-1}[(x + iy)/c] \text{ and } z = z.$$

Explicitly, we have

$$x = c\cosh\xi, \; y = c\sinh\xi, \; z = z \text{ and } h^{-2} = c^2\cosh 2\xi/2.$$

The curves $\eta = \text{constant}$ represent a family of confocal hyperbolas while the curves $\xi = \text{constant}$ represent a family of the confocal ellipse. The length $2c$ is the distance between their common foci. Both sets of curves intersect each other orthogonally at every point in space. The parameter ξ varies from a where it defines the interfocal line to b and $z \in (0, \ell)$. The scale factors

$$h_i \; (i = \xi, z) \text{ in } ds^2 = (h_\xi \, d\xi)^2 + (h_z \, dz)^2,$$

are given by

$$h_\xi^2 = c^2 J^2, \; h_z = 1; \; J^2 = (1/2)\cosh 2\xi.$$

2.2. Basic equations

Now the basic equations of strain displacement relations, stress-strain relations for a functionally graded hollow elliptic-cylinder are given by

$$\varepsilon_{\xi\xi} = \frac{1}{c\cosh\xi}\frac{\partial u_\xi}{\partial\xi}, \varepsilon_{\eta\eta} = \frac{1}{c\cosh\xi}u_\xi, \varepsilon_{zz} = \frac{\partial u_z}{\partial z}. \tag{1}$$

Furthermore, the thermal stress components in terms of strain are given as

$$\left.\begin{array}{l} \sigma_{\xi\xi} = \lambda(\xi)(\varepsilon_{\xi\xi} + \varepsilon_{\eta\eta} + \varepsilon_{zz}) + 2\mu(\xi)\varepsilon_{\xi\xi} - [3\lambda(\xi) + 2\mu(\xi)]\alpha(\xi)\Delta T \\ \sigma_{\eta\eta} = \lambda(\xi)(\varepsilon_{\xi\xi} + \varepsilon_{\eta\eta} + \varepsilon_{zz}) + 2\mu(\xi)\varepsilon_{\eta\eta} - [3\lambda(\xi) + 2\mu(\xi)]\alpha(\xi)\Delta T \\ \sigma_{zz} = \lambda(\xi)(\varepsilon_{\xi\xi} + \varepsilon_{\eta\eta} + \varepsilon_{zz}) + 2\mu(\xi)\varepsilon_{zz} - [3\lambda(\xi) + 2\mu(\xi)]\alpha(\xi)\Delta T \end{array}\right\}, \tag{2}$$

in which $\varepsilon_{\xi\xi}, \varepsilon_{\eta\eta}, \varepsilon_{zz}$ are the strain components, υ is Poisson's ratio, $E(\xi)$ is the modulus of elasticity, $\Delta T = T_R - T_S$, T_R is the reference temperature and T_S is the surrounding temperature, $\alpha(\xi)$ represents the coefficient of thermal expansion of the material, and Lame's constants are given by

$$\lambda(\xi) = \frac{\upsilon E(\xi)}{(1+\upsilon)(1-2\upsilon)}, \; \mu(\xi) = \frac{E(\xi)}{(1+\upsilon)}.$$

The Navier–Stokes equation can be obtained in terms of strain components as

$$\begin{array}{l} (\varepsilon_{\xi\xi} + \varepsilon_{\eta\eta} + \varepsilon_{zz})\,\text{grad}[\lambda(\xi)] + 2\varepsilon_{\eta\eta}\,\text{grad}[\mu(\xi)] + [\lambda(\xi) + 2\mu(\xi)] \\ \times \text{grad div}\,\vec{u} - \mu(\xi)\,\text{curl curl}\,\vec{u} = \text{grad}[(3\lambda(\xi) + 2\mu(\xi))\alpha(\xi)\Delta T]. \end{array} \tag{3}$$

Manthena et al.: Thermal stress analysis in a functionally graded hollow elliptic

AAM: Intern. J., Vol 12, Issue 1 (June 2017)   617

Substituting Equation (1) in Equations (3), we obtain the expressions for the complete Navier–Stokes equation in terms of displacement as

$$
\frac{1}{c\cosh\xi} \frac{\upsilon\,E'(\xi)}{(1+\upsilon)(1-2\upsilon)}\left[\frac{1}{c\cosh\xi}\frac{du_{\xi}}{d\xi} + \frac{1}{c\cosh\xi}u_{\xi} + \frac{du_{z}}{dz}\right]
$$
$$
+ \frac{1}{c\cosh\xi}u_{\xi}\frac{1}{c\cosh\xi}\frac{E'(\xi)}{(1+\upsilon)} + \frac{E(\xi)(1-\upsilon)}{(1+\upsilon)(1-2\upsilon)}\frac{1}{c\cosh\xi}
$$
$$
\times\frac{d}{d\xi}\left[\frac{1}{c\cosh\xi}\frac{du_{\xi}}{d\xi} + \frac{1}{c\cosh^{2}\xi}u_{\xi} + \frac{du_{z}}{dz}\right] \tag{4}
$$
$$
= \frac{1}{c\cosh\xi}\frac{d}{d\xi}\left[\frac{E(\xi)}{(1-2\upsilon)}\alpha(\xi)\Delta T\right].
$$

2.3. Boundary conditions

For a complete solution to the thermoelastic problem, displacement field is to be determined such that for $T \neq 0$, there is zero traction on all surfaces of the hollow elliptic cylinder. Thus, we assume the following conditions as

a. Zero traction conditions on the inner and outer curved surfaces

$$
\sigma_{\xi\eta} = 0, \; \sigma_{\xi z} = 0 \text{ at } \xi = a, b. \tag{5}
$$

b. For the hollow cylinder subjected to time dependent pressures $P_i(t)$ and $P_O(t)$ on the inner and outer surfaces, the mechanical boundary conditions can be expressed as

$$
\sigma_{\xi\xi}\big|_{\xi=a} = P_i(t), \qquad \sigma_{\xi\xi}\big|_{\xi=b} = P_o(t). \tag{6}
$$

c. Zero normal force on $z = 0, \ell$:

$$
2\pi\int_a^b\sigma_{zz}\,\xi\,d\xi = 0. \tag{7}
$$

d. Boundary conditions of the finite-length cylinder is assumed to be simply supported at the two longitudinal edges, i.e.,

$$
u_{\xi} = 0, \; \sigma_{zz} = 0, \; \sigma_{\eta z} = 0, \; \sigma_{\xi z} = 0 \text{ at } z = 0, \ell. \tag{8}
$$

The Equations (1) to (8) constitute the mathematical formulation of the problem under consideration.

3. Reformulation of the problem

We consider the case in which the functionally graded material with non-constant elastic parameters material properties vary radially according to exponential law as

$$E(\xi) = E_0 \exp(m_1 \xi),\, \alpha(\xi) = \alpha_0 \exp(m_2 \xi). \tag{9}$$

where E_0 and α_0 are the reference values of modulus of elasticity and coefficient of thermal expansion respectively, m_1 and m_2 are the material parameters whose combination forms a wide range of nonlinear and continuous profiles to describe the reasonable variation of material constants and thermal expansion coefficients.

In order to solve the fundamental Equation (4) taking into account Equation (9), we introduce a new function as

$$u_\eta(\eta) = 0,\; u_z(z) = Gz. \tag{10}$$

in which G is the unknown constant (that is, independent of variable ξ) and to be determined. The term $u_\xi(\xi)$ represents a radial expansion or contraction in which, in general, the inner and outer radii change, but angle remains constant and $u_z(z) = Gz$ is a uniform axial extension or contraction.

4. Solution of the problem

The governing Equation (4) can be reformulated by taking into account Equation (9) and Equation (10), we obtain the differential equation in the following form

$$\frac{d^2 u_\xi}{d\xi^2} + A_1 \frac{du_\xi}{d\xi} + A_2\, u_\xi = A_3 \exp[m_2 \xi] \cosh \xi - A_4 \cosh \xi. \tag{11}$$

in which

$$A_1 = \left(1 + \frac{m_1 \nu}{(1-\nu)}\right),\; A_2 = (m_1 - 2),\; A_3 = \frac{c\alpha_0(m_1 + m_2)(1+\nu)}{(1-\nu)},\; A_4 = \frac{cGm_1\nu}{(1-\nu)}.$$

Equation (10) is a second order differential equation whose solution is given by

$$u_\xi = C_1 \exp(B_1 \xi) + C_2 \exp(B_2 \xi) + B_3 \exp[(1 + m_2)\xi]$$
$$+ B_4 \exp[(-1 + m_2)\xi] - B_5 \exp(\xi) - B_6 \exp(-\xi). \tag{12}$$

in which

Manthena et al.: Thermal stress analysis in a functionally graded hollow elliptic

AAM: Intern. J., Vol 12, Issue 1 (June 2017)   619

$$B_1 = [-A_1 - (A_1^2 - 4A_2)^{1/2}]/2, \quad B_2 = [-A_1 + (A_1^2 - 4A_2)^{1/2}]/2,$$

$$B_3 = A_3[1/(m_2^2 + (2+A_1)m_2 + 1 + A_1 + A_2)]/2,$$

$$B_4 = A_3[1/(m_2^2 + (-2+A_1)m_2 + 1 - A_1 + A_2)]/2,$$

$$B_5 = A_4[1/(1+A_1+A_2)]/2, \quad B_6 = A_4[1/(1-A_1+A_2)]/2.$$

By substituting Equation (12) in (2), the stress components are obtained as

$$
\begin{aligned}
\sigma_{\xi\xi} = &(E_0 \exp(m_1\xi)/(1+\upsilon))\{[(\upsilon/((1-2\upsilon)c\cosh\xi))(C_1(1+B_1)\exp(B_1\xi) \\
&+ C_2(1+B_2)\exp(B_2\xi) + B_3(2+m_2)\exp((1+m_2)\xi) \\
&+ B_4 m_2 \exp((-1+m_2)\xi) - 2B_5 \exp(\xi))] + [\upsilon G z/(1-2\upsilon)] + [(2/c\cosh\xi) \\
&\times (C_1 B_1 \exp(B_1\xi) + C_2 B_2 \exp(B_2\xi) + B_3(1+m_2)\exp((1+m_2)\xi) \\
&+ B_4(-1+m_2)\exp((-1+m_2)\xi) - B_5 \exp(\xi) + B_6 \exp(-\xi))] \\
&- [((2-\upsilon)/(1-2\upsilon))(\alpha_0 \exp(m_2\xi)\Delta T)]\},
\end{aligned}
\tag{13}
$$

$$
\begin{aligned}
\sigma_{\eta\eta} = &(E_0 \exp(m_1\xi)/(1+\upsilon))\{[(\upsilon/((1-2\upsilon)c\cosh\xi))(C_1(1+B_1)\exp(B_1\xi) \\
&+ C_2(1+B_2)\exp(B_2\xi) + B_3(2+m_2)\exp((1+m_2)\xi) \\
&+ B_4 m_2 \exp((-1+m_2)\xi) - 2B_5 \exp(\xi))] + [\upsilon G z/(1-2\upsilon)] + [(2/c\cosh\xi) \\
&\times (C_1 \exp(B_1\xi) + C_2 \exp(B_2\xi) + B_3 \exp((1+m_2)\xi) + B_4 \exp((-1+m_2)\xi) \\
&- B_5 \exp(\xi) - B_6 \exp(-\xi))] \\
&- [((2-\upsilon)/(1-2\upsilon))(\alpha_0 \exp(m_2\xi)\Delta T)]\},
\end{aligned}
\tag{14}
$$

$$
\begin{aligned}
\sigma_{zz} = &(E_0 \exp(m_1\xi)/(1+\upsilon))\{[(\upsilon/((1-2\upsilon)c\cosh\xi))(C_1(1+B_1)\exp(B_1\xi) \\
&+ C_2(1+B_2)\exp(B_2\xi) + B_3(2+m_2)\exp((1+m_2)\xi) \\
&+ B_4 m_2 \exp((-1+m_2)\xi) - 2B_5 \exp(\xi))] + [\upsilon G z/(1-2\upsilon)] + [2G] \\
&- [((2-\upsilon)/(1-2\upsilon))(\alpha_0 \exp(m_2\xi)\Delta T)]\}.
\end{aligned}
\tag{15}
$$

4.1. Further investigation:

(i) The homogeneous case

For $m_1 = 0$ and $m_2 = 0$, one obtains all material constants of the Equation (9) that are independent of radial coordinates, then $E(\xi) = E_0$ and $\alpha(\xi) = \alpha_0$. Using Equation (13) in Equation (6), the constants C_1 and C_2 are obtained as

$$C_1 = \frac{\Delta_{13}\Delta_{15} - \Delta_{12}\Delta_{16}}{\Delta_{11}\Delta_{15} - \Delta_{12}\Delta_{14}}, \quad C_2 = \frac{\Delta_{11}\Delta_{16} - \Delta_{13}\Delta_{14}}{\Delta_{11}\Delta_{15} - \Delta_{12}\Delta_{14}}, \tag{16}$$

where

$$\Delta_{11} = (\exp(B_1 a)/c\cosh a)((\nu(1+B_1)/(1-2\nu))+2B_1),$$
$$\Delta_{12} = (\exp(B_2 a)/c\cosh a)((\nu(1+B_2)/(1-2\nu))+2B_2),$$
$$\Delta_{13} = -D_{11}-D_{12}-D_{13}+D_{14}+D_{15},$$
$$D_{11} = (\nu/(1-2\nu)c\cosh a)[2B_3\exp(a)-2B_5\exp(a)],$$
$$D_{12} = \nu G z/(1-2\nu),$$
$$D_{13} = 2[B_3\exp(a)-B_4\exp(-a)-B_5\exp(a)+B_6\exp(a)]/(c\cosh a),$$
$$D_{14} = ((2-\nu)/(1-2\nu))\alpha_0\Delta T,$$
$$D_{15}(t) = -(1+\nu)P_i(t)/E_0,$$
$$\Delta_{14} = [\exp(B_1 b)/c\cosh b][(\nu(1+B_1)/(1-2\nu))+2B_1],$$
$$\Delta_{15} = [\exp(B_2 b)/c\cosh b][(\nu(1+B_2)/(1-2\nu))+2B_2],$$
$$\Delta_{16} = -J_{11}-J_{12}-J_{13}+J_{14}+J_{15},$$
$$J_{11} = [\nu/(1-2\nu)c\cosh b][2B_3\exp(b)-2B_5\exp(b)],$$
$$J_{12} = \nu G z/(1-2\nu),$$
$$J_{13} = 2[B_3\exp(b)-B_4\exp(b)-B_5\exp(b)+B_6\exp(b)]/(c\cosh b),$$
$$J_{14} = [(2-\nu)/(1-2\nu)]\alpha_0\Delta T,$$
$$J_{15} = -(1+\nu)P_o(t)/E_0.$$

Using Equation (15) in Equation (8), we get

$$G = [(1-2\nu)/(\nu h+2-4\nu)](E_{12}-E_{11}), \tag{17}$$

where

$$E_{11} = \{\upsilon/[(1-2\upsilon)c\cosh(h)]\}(C_1(1+B_1)\exp(B_1 h)+C_2(1+B_2)\exp(B_2 h)$$
$$\qquad +2B_3\exp(h)-2B_5\exp(h)),$$
$$E_{12} = \alpha_0[(2-\upsilon)/(1-2\upsilon)]\Delta T.$$

(ii) The inhomogeneous case

For the inhomogeneity parameter $m_1 \neq 0$ and $m_2 \neq 0$, the radial stress expression (13) can be utilized taking into account the thermo-mechanical boundary conditions (6) for obtaining the constants C_1 and C_2 as

$$C_1 = \frac{\Delta_{23}\Delta_{25}-\Delta_{22}\Delta_{26}}{\Delta_{21}\Delta_{25}-\Delta_{22}\Delta_{24}}, \quad C_2 = \frac{\Delta_{21}\Delta_{26}-\Delta_{23}\Delta_{24}}{\Delta_{21}\Delta_{25}-\Delta_{22}\Delta_{24}}, \tag{18}$$

where

Manthena et al.: Thermal stress analysis in a functionally graded hollow elliptic

AAM: Intern. J., Vol 12, Issue 1 (June 2017)   621

$$\Delta_{21} = (\exp(B_1 a)/c\cosh a)((\nu(1+B_1)/(1-2\nu))+2B_1),$$

$$\Delta_{22} = (\exp(B_2 a)/c\cosh a)((\nu(1+B_2)/(1-2\nu))+2B_2),$$

$$\Delta_{23} = -D_{21} - D_{22} - D_{23} + D_{24} + D_{25},$$

$$D_{21} = (\nu/(1-2\nu)c\cosh a)[B_3(2+m_2)\exp((1+m_2)a)$$
$$+ B_4 m_2 \exp((-1+m_2)a) - 2B_5 \exp(a)],$$

$$D_{22} = (\nu G z/(1-2\nu)),$$

$$D_{23} = (2/(c\cosh a))[B_3(1+m_2)\exp((1+m_2)a) + B_4(-1+m_2)$$
$$\times \exp((-1+m_2)a) - B_5 \exp(a) + B_6 \exp(a)],$$

$$D_{24} = ((2-\nu)/(1-2\nu))\alpha_0 \exp(m_2 a)\Delta T,$$

$$D_{25} = [-(1+\nu)P_i(t)/E_0 \exp(m_1 a)],$$

$$\Delta_{24} = (\exp(B_1 b)/c\cosh b)\times((\nu(1+B_1)/(1-2\nu))+2B_1),$$

$$\Delta_{25} = (\exp(B_2 b)/c\cosh b)\times((\nu(1+B_2)/(1-2\nu))+2B_2),$$

$$\Delta_{26} = -J_{21} - J_{22} - J_{23} + J_{24} + J_{25},$$

$$J_{21} = (\nu/(1-2\nu)c\cosh b)[B_3(2+m_2)\exp((1+m_2)b)$$
$$+ B_4 m_2 \exp((-1+m_2)b) - 2B_5 \exp(b)],$$

$$J_{22} = (\nu G z/(1-2\nu)),$$

$$J_{23} = (2/(c\cosh b))[B_3(1+m_2)\exp((1+m_2)b) + B_4(-1+m_2)$$
$$\times \exp((-1+m_2)b) - B_5 \exp(b) + B_6 \exp(b)],$$

$$J_{24} = ((2-\nu)/(1-2\nu))\times\alpha_0 \exp(m_2 b)\Delta T,$$

$$J_{25} = [-(1+\nu)P_o(t)/E_0 \exp(m_1 b)].$$

For the nonhomogeneous hollow cylinder, we consider the normal force condition (7) as

$$2\pi \int_a^b \left\{ \begin{array}{l} (E_0 \exp(m_1 \xi)/(1+\upsilon))\{[(\upsilon/((1-2\upsilon)c\cosh \xi))(C_1(1+B_1)\exp(B_1\xi) \\ + C_2(1+B_2)\exp(B_2\xi) + B_3(2+m_2)\exp((1+m_2)\xi) \\ + B_4 m_2 \exp((-1+m_2)\xi) - 2B_5 \exp(\xi))] + [\upsilon G z/(1-2\upsilon)] + [2G] \\ - [((2-\upsilon)/(1-2\upsilon))(\alpha_0 \exp(m_2\xi)\Delta T)]\} \end{array} \right\} \xi\, d\xi = 0. \quad (19)$$

Using Equations (7) and (19), the value of unknown coefficient G can be calculated. Since the expression of G obtained so was very large, we have not mentioned it here. However, the value of G was obtained by means of Mathematica software for numerical computations.

4.2. Transition to circular plate

When the semi major axis of an elliptic-cylinder degenerates into circular cylinder, we find that internal radius a, outer radius $b \to \infty$, occupies the space

$$D' = \{(r,z) \in R^2 : a < r < b, 0 \le z \le \ell\}.$$

For that we take

$$e \to 0 \ as \ \xi \to +\infty, \ h\cosh\xi \to r, \ i.e \ (1/2)h\exp(\xi) \to r, l \to 0.$$

Hence, Equation (12) degenerates into the hollow circular cylinder for which the solution of displacement function is as follows.

$$u_r = C_1 \, r^{B_1} + C_2 \, r^{B_2} + B_3 r^{(1+m_2)} + B_4 r^{(-1+m_2)} - B_5 \, r - B_6 (1/r).$$

This result agrees with Chen et al. (2002).

5. Numerical results and discussion

The numerical computations are carried out for ceramic-metal-based FGM, in which zirconia is selected as ceramic and aluminium as metal, with non-dimensional variables as given below.

$$\chi = \frac{\xi}{l}, \quad \zeta = \frac{z}{l}, \quad \bar{u}_\xi = \frac{u_\xi}{\theta_R l}, \quad (\bar{\sigma}_{\xi\xi}, \bar{\sigma}_{\eta\eta}, \bar{\sigma}_{zz}) = \frac{(\sigma_{\xi\xi}, \sigma_{\eta\eta}, \sigma_{zz})}{E\alpha_0\theta_R}, \quad \tau = \frac{\kappa t}{l^2}.$$

with parameters $a = 2 \, cm, b = 4 \, cm, l = 2cm$, reference temperature $T_R = 330^O K$, surrounding temperature $T_S = 300^O K$.

The pressures on the inner and outer surfaces are taken as

$$P_i(t) = -Q_1 (1 - \cos(\varpi_1 t)) \text{ and } P_o(t) = -Q_2 (1 - \cos(\varpi_2 t)).$$

Table 1. Thermo-mechanical properties of Zirconia and Aluminium at room temperature

Property	Zirconia (Ceramic)	Aluminium (Metal)
Thermal conductivity $\lambda_i \, [W/cmK]$	0.282	0.901
Thermal diffusivity $\kappa_i \, [\times 10^{-6} cm^2/s]$	0.083	0.223
Thermal expansion coefficient $\alpha_i \, [\times 10^{-6}/K]$	5.4	14.0
Young's modulus $E_i \, [N/cm^2]$	36×10^6	21.8×10^6
Poisson's ratio $\upsilon_i \, [-]$	0.23	0.31

5.1. Time $\tau = 0$ in pressure load

The following Figures (1 to 8) are plotted by taking time $\tau = 0$.

Manthena et al.: Thermal stress analysis in a functionally graded hollow elliptic

AAM: Intern. J., Vol 12, Issue 1 (June 2017)   623

The figures on the left are of homogeneous elliptic-cylinder in which $m_1 = m_2 = 0$, while those on the right are of nonhomogeneous elliptic-cylinder in which $m_1 \neq 0$, $m_2 \neq 0$.
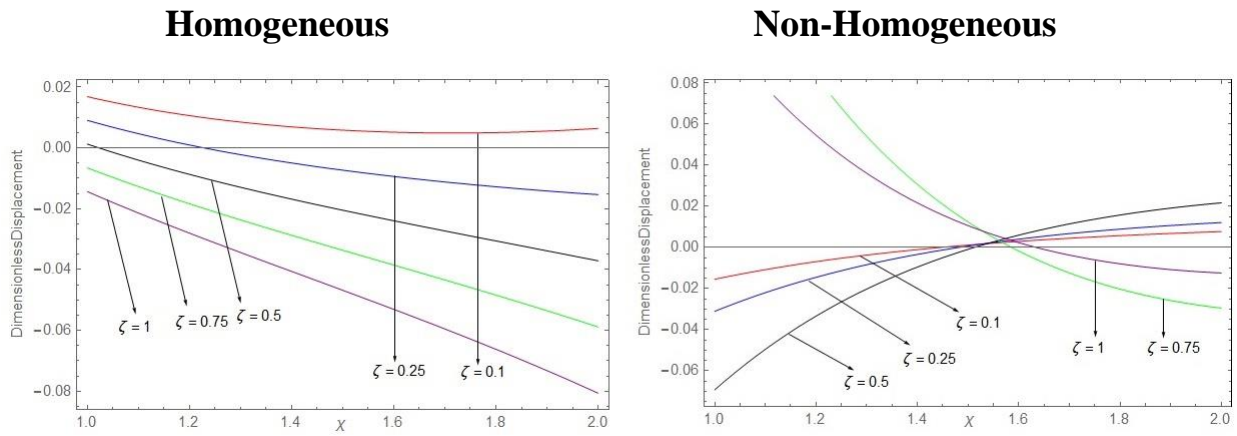
Homogeneous   **Non-Homogeneous**

Figure 1. Variation of dimensionless displacement along χ
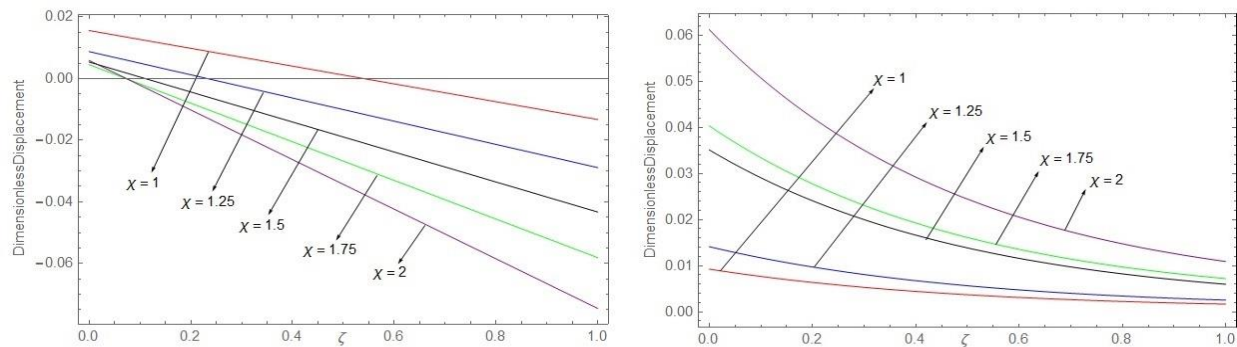
Figure 2. Variation of dimensionless displacement along ζ

Figure 1 shows the variation of dimensionless displacement along the radial direction for different values of $\zeta = 0.1, 0.25, 0.5, 0.75, 1$. It is seen that the nature is linear. For homogeneous elliptic-cylinder, the absolute value of displacement is low at the curved surface and is gradually increasing towards the centre. For nonhomogeneous elliptic-cylinder, the absolute value of displacement is low at the curved surface and is gradually increasing towards the centre and is peak at $\chi = 1.1$ for $\zeta = 0.75, 1$, while it is high at the curved surface and is decreasing towards the centre for the remaining values of ζ.

Figure 2 shows the variation of dimensionless displacement along the axial direction for different values of $\chi = 1, 1.25, 1.5, 1.75, 2$. In the homogeneous case, the absolute value of displacement is high at the upper surface and is gradually increasing towards the lower surface. Also it is peak at the central part. In the nonhomogeneous case, the absolute value of displacement is positive throughout and is becoming high to low from the lower to the upper surface.
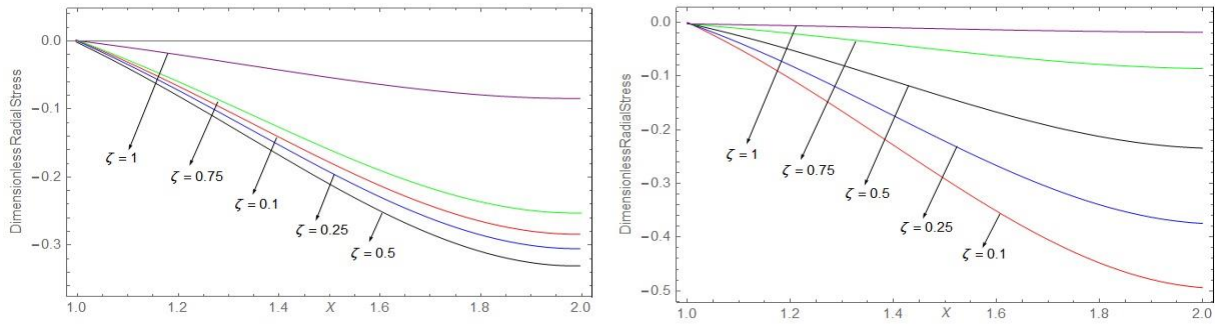
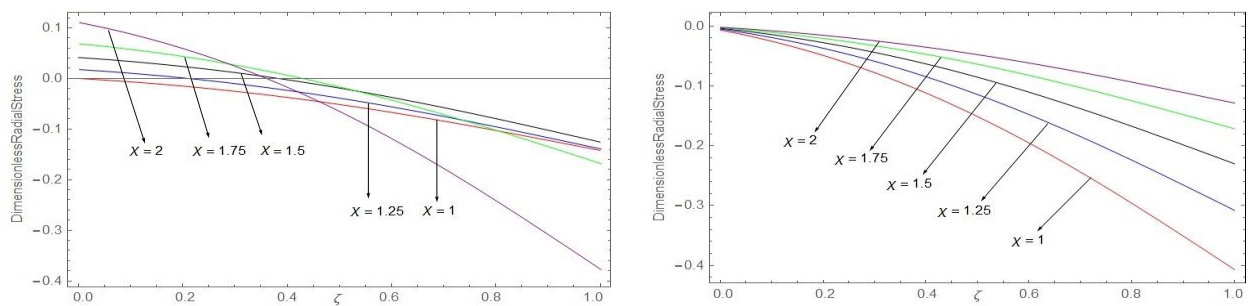**Figure 3.** Variation of dimensionless radial stress along χ

Figure 4. Variation of dimensionless radial stress along ζ

Figure 3 shows the variation of dimensionless radial stress along the radial direction for different values of ζ. In the homogeneous case, the radial stress is compressive. The absolute value of radial stress is gradually increasing from the curved surface towards the centre of the elliptic-cylinder. Its magnitude is moderate at $\zeta = 0.1$, low at $\zeta = 0.5$ and high at $\zeta = 1$. In the nonhomogeneous case, it is increasing from the curved surface towards the centre.

Figure 4 shows the variation of dimensionless radial stress along the axial direction for different values of χ. In the homogeneous case, the radial stress is tensile in the region $0 \le \zeta \le 0.22$, $0 \le \zeta \le 0.37$ and $0 \le \zeta \le 0.42$ for $\chi = 1.25$, $\chi = 1.5, 2$ and $\chi = 1.75$ respectively, whereas compressive in the remaining region. The magnitude is high at the lower surface and is decreasing towards the upper surface. In the nonhomogeneous case, the absolute value of radial stress is slowly decreasing from the lower to the upper surface.
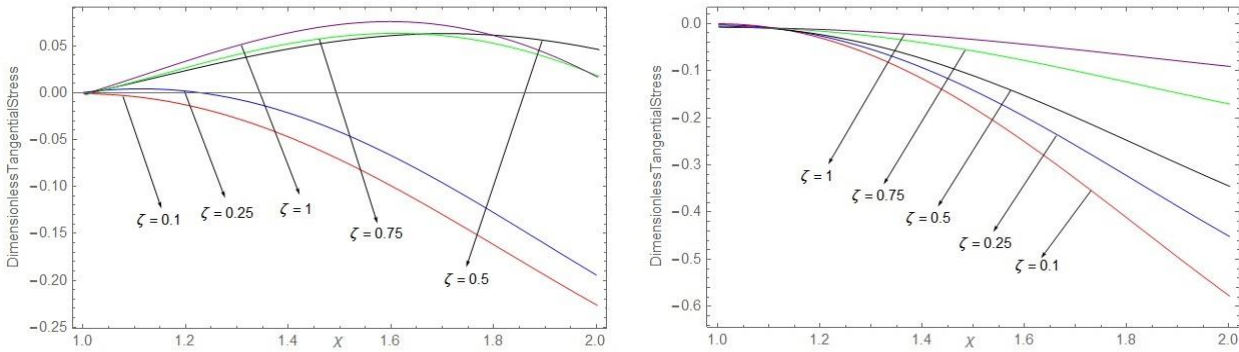
Manthena et al.: Thermal stress analysis in a functionally graded hollow elliptic

AAM: Intern. J., Vol 12, Issue 1 (June 2017) 625

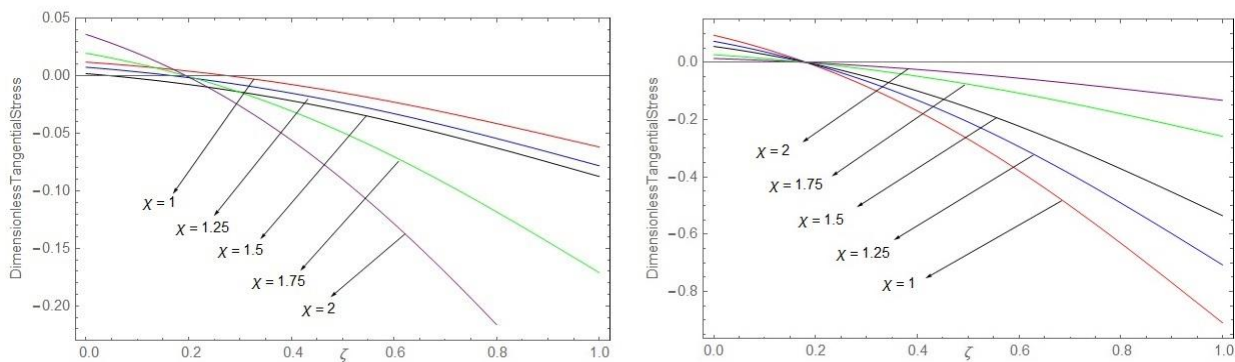**Figure 5.** Variation of dimensionless tangential stress along χ

Figure 6. Variation of dimensionless tangential stress along ζ

Figure 5 shows the variation of dimensionless tangential stress the along radial direction for different values of ζ. In the homogeneous case, the tangential stress is tensile for $\zeta = 0.5, 0.75, 1$ with peak value at $\chi = 1.6$ and compressive for $\zeta = 0.1, 0.25$. The absolute value of tangential stress is very low at the curved surface. In the nonhomogeneous case, it is steady until $\chi = 1.2$ and then gradually decreasing towards the curved surface. Also, the magnitude is low at $\zeta = 0.1$ and is increasing with the increase in ζ.

Figure 6 shows the variation of dimensionless tangential stress along the axial direction for different values of χ. In the homogeneous case, the tangential stress is tensile in the region $0 \leq \zeta \leq 0.15$, $0 \leq \zeta \leq 0.2$ and $0 \leq \zeta \leq 0.3$ for $\chi = 1.25$, $\chi = 1.75, 2$ and $\chi = 1$ respectively, whereas compressive in the remaining region. Also, the absolute value is decreasing towards the upper surface. In the nonhomogeneous case, it is tensile in the region $0 \leq \zeta \leq 0.2$, whereas compressive in the remaining region. We also observe that the magnitude is low in the nonhomogeneous case as compared to that of the homogeneous case.
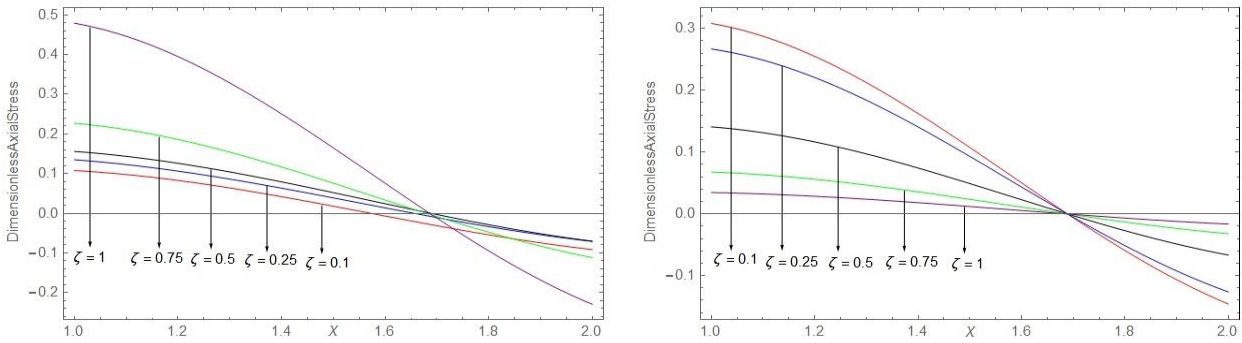
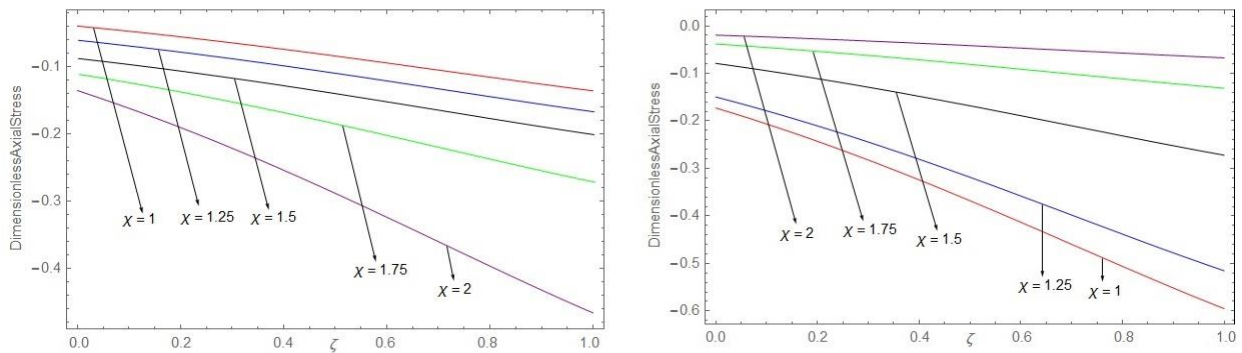**Figure 7.** Variation of dimensionless axial stress along χ

Figure 8. Variation of dimensionless axial stress along ζ

Figure 7 shows the variation of dimensionless axial stress along the radial direction for different values of ζ. In the homogeneous case, the axial stress is tensile in the region $1 \leq \chi \leq 1.57$ and $1 \leq \chi \leq 1.7$ for $\zeta = 0.1$ and $\zeta = 0.25, 0.5, 0.75, 1$ respectively, whereas compressive in the remaining region. The axial stress is peak and low at the central part and curved surface respectively for all ζ, but it is very high and low at the central part and curved surface for $\zeta = 1$, as compared to the other value of ζ. In the nonhomogeneous case, it is tensile in the region $1 \leq \chi \leq 1.7$, whereas compressive in the remaining region for all ζ.

Figure 8 shows the variation of dimensionless axial stress along the axial direction for different values of χ. In the homogeneous case, the axial stress is compressive throughout. Also, the absolute value is linearly decreasing from the lower to the upper surface. Also, the magnitude is more for $\chi = 1$ and is decreasing with increase in χ. In the nonhomogeneous case, we observe that it is linearly decreasing from the lower to the upper surface, while the magnitude is more for $\chi = 2$ and is decreasing with a decrease in χ.

5.2. Time $\tau = 2$ in pressure load

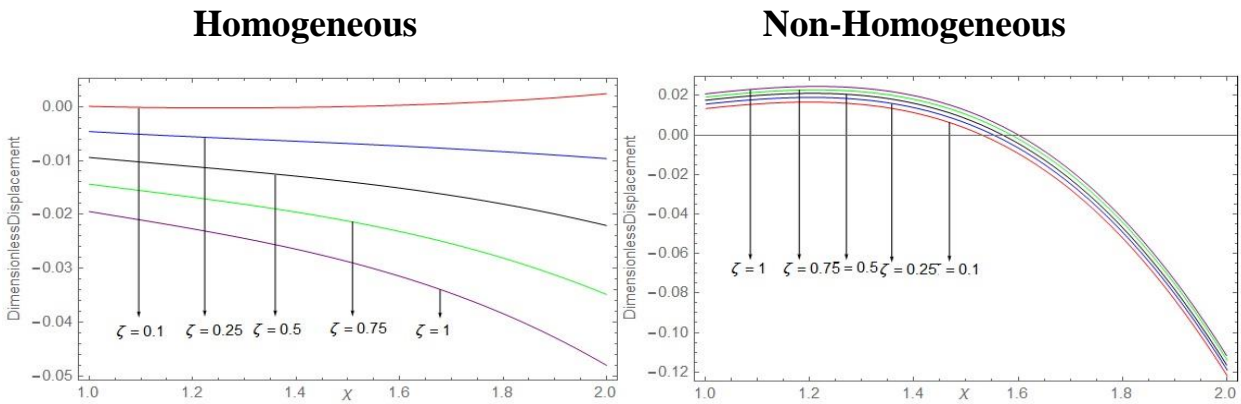The following Figures (9 to 16) are plotted by taking time $\tau = 2$.

Manthena et al.: Thermal stress analysis in a functionally graded hollow elliptic

AAM: Intern. J., Vol 12, Issue 1 (June 2017)   627

Homogeneous   **Non-Homogeneous**

Figure 9. Variation of dimensionless displacement along χ
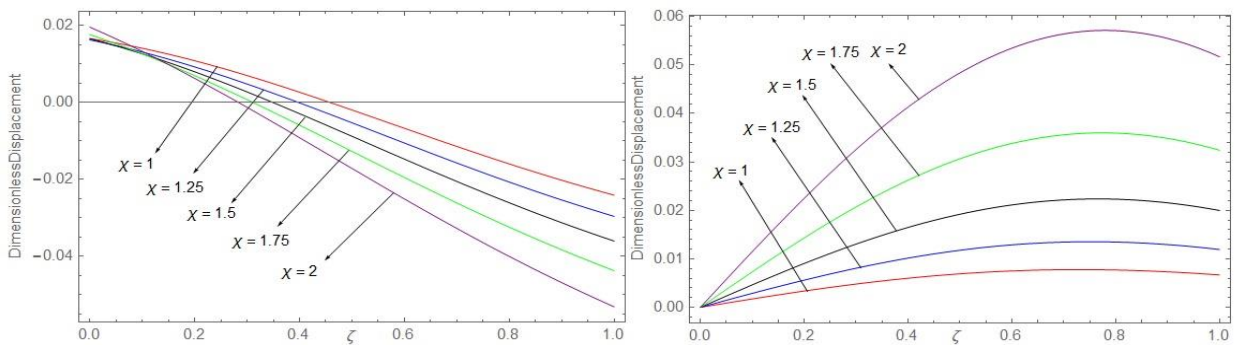
Figure 10. Variation of dimensionless displacement along ζ

Figure 9 shows the variation of dimensionless displacement along the radial direction for different values of ζ. For nonhomogeneous elliptic-cylinder, the displacement is observed to decay exponentially from the center towards the outer radius.

Figure 10 shows the variation of dimensionless displacement along the axial direction for different values of χ. In the homogeneous case, the absolute value of displacement is high at the upper surface and is linearly decreasing towards the lower surface. In the nonhomogeneous case, the displacement is positive throughout and is sinusoidal in nature.
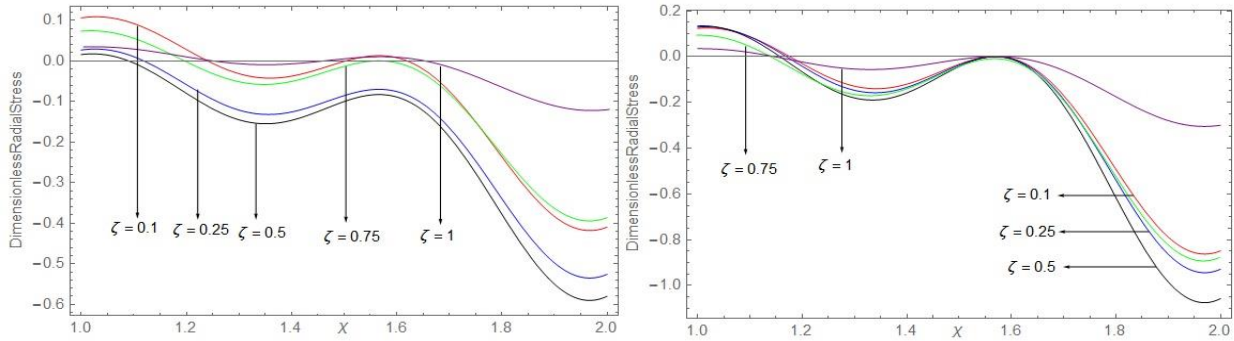
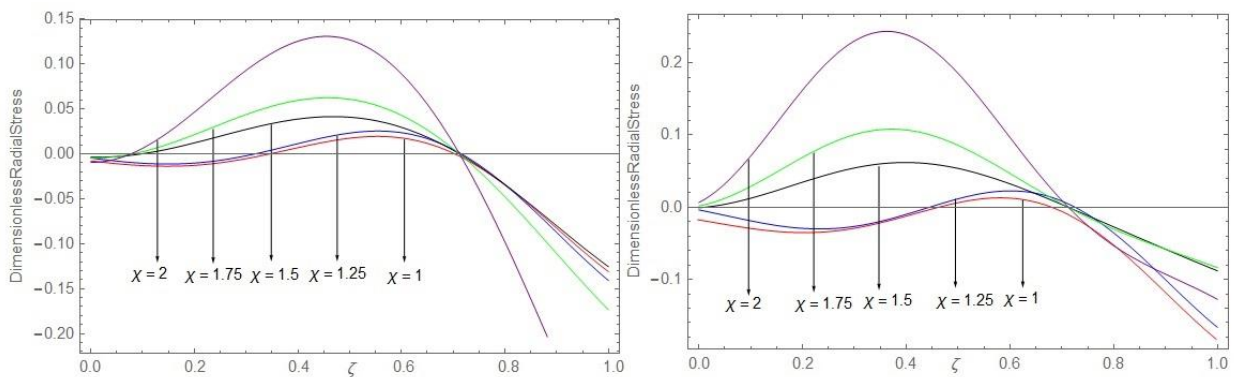**Figure 11.** Variation of dimensionless radial stress along χ

Figure 12. Variation of dimensionless radial stress along ζ

Figure 11 shows the variation of dimensionless radial stress along the radial direction for different values of ζ. For both the homogeneous and nonhomogeneous cases, the radial stress is tensile near the center and is compressive in the remaining region. Also, the magnitude is more at $\zeta = 0.1,1$, as compared to remaining values of ζ.

Figure 12 shows the variation of dimensionless radial stress along the axial direction for different values of χ. The radial stress is tensile in the region $0.1 < \zeta < 0.7$, whereas compressive in the remaining regions. Also, the magnitude is low in the homogeneous case as compared to the nonhomogeneous case.
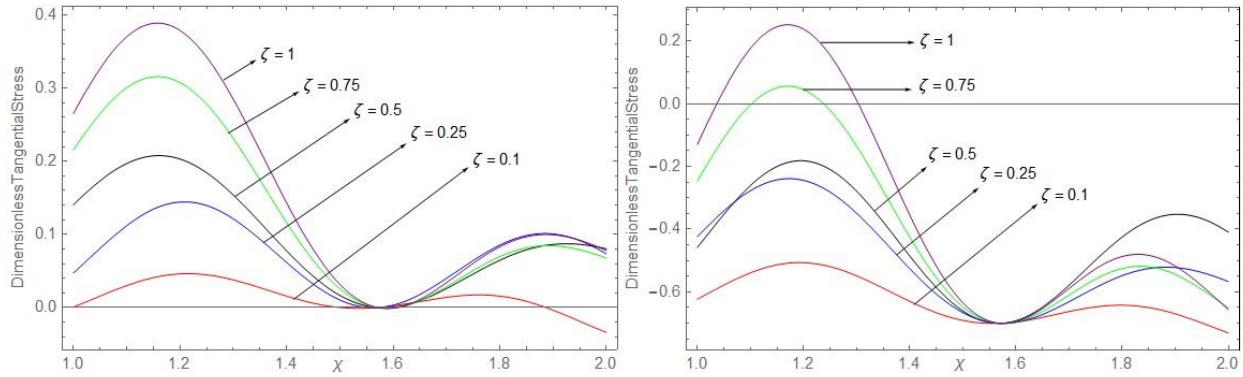
Manthena et al.: Thermal stress analysis in a functionally graded hollow elliptic

AAM: Intern. J., Vol 12, Issue 1 (June 2017)   629

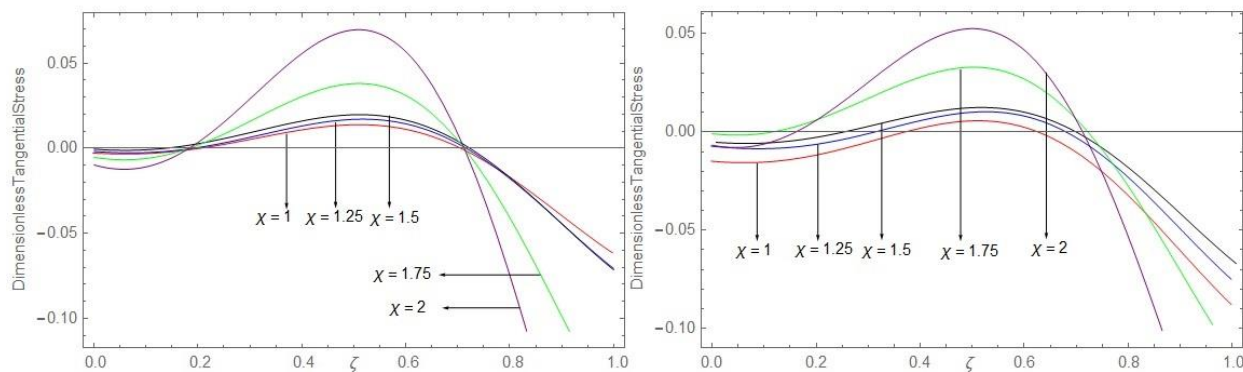**Figure 13.** Variation of dimensionless tangential stress along χ

Figure 14. Variation of dimensionless tangential stress along ζ

Figure 13 shows the variation of dimensionless tangential stress along the radial direction for different values of ζ. It is seen that nature is sinusoidal. In the homogeneous case, the tangential stress is tensile throughout, while in the nonhomogeneous case it is tensile near the inner radius for $\zeta = 0.75,1$, whereas compressive in the remaining region.

Figure 14 shows the variation of dimensionless tangential stress along the axial direction for different values of χ. For both the homogeneous and nonhomogeneous cases, the tangential stress is tensile in the region $0.2 \leq \zeta \leq 0.7$, whereas compressive in the remaining regions.
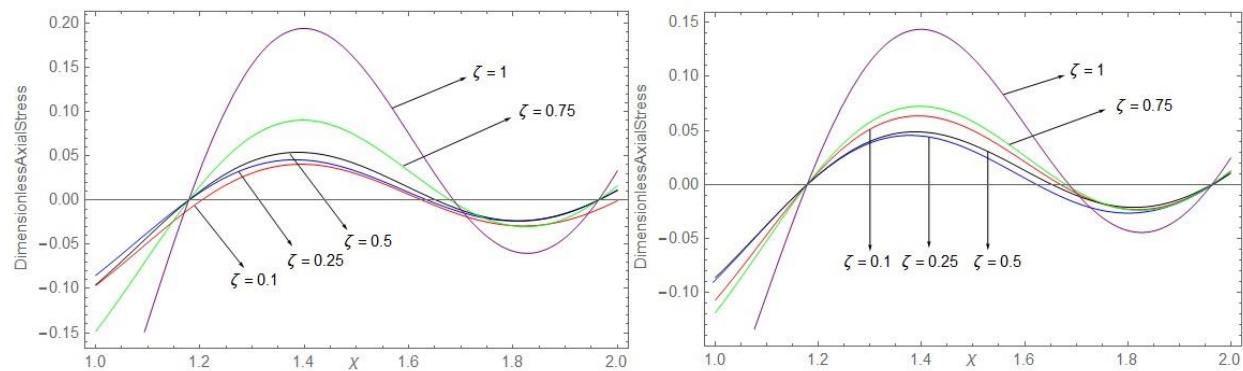

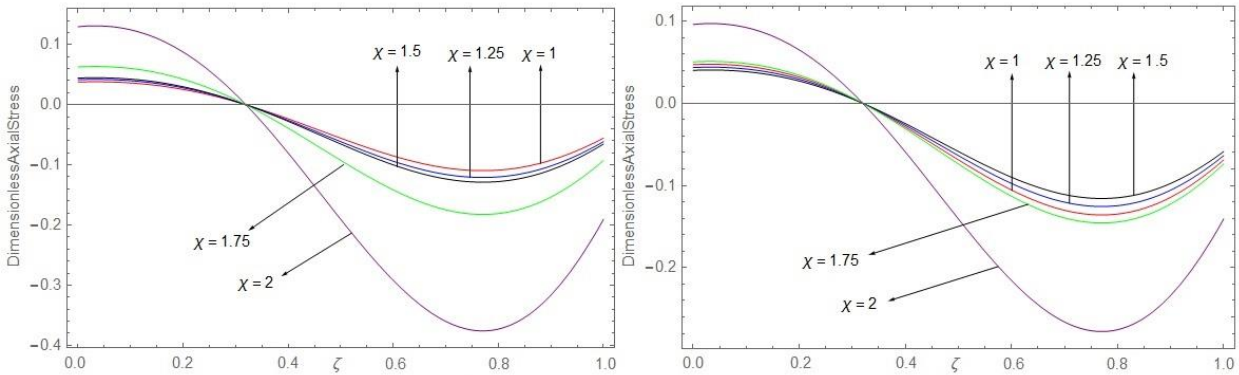**Figure 15.** Variation of dimensionless axial stress along χ

Figure 16. Variation of dimensionless axial stress along ζ

Figure 15 shows the variation of dimensionless axial stress along the radial direction for different values of ζ. The axial stress is tensile in the region $1.2 \leq \chi \leq 1.7$, whereas compressive in the remaining regions. The axial stress reaches the peak value at $\chi = 1.4$. Also, the magnitude is low in the nonhomogeneous case as compared to that of the homogeneous case.

Figure 16 shows the variation of dimensionless axial stress along the axial direction for different values of χ. The axial stress is tensile in the region $0 \leq \zeta \leq 0.3$, whereas compressive in the remaining region. Also, it is converging to zero at $\zeta = 0.3$.

6. Conclusion

In the present paper, we have investigated displacement and thermal stresses in a thick hollow elliptic-cylinder subjected to uniform heating. The material properties except for Poisson's ratio and density are considered to vary by exponential law along the axial direction. Furthermore, the influence of homogeneity and inhomogeneity grading is investigated by changing parameters m_1, m_2.

During this investigation, the following results are obtained.

(1) The nature of displacement and all stresses is found to be linear when plotted along radial and axial directions for a time $\tau = 0$, whereas all the stresses are found to be sinusoidal for a time $\tau = 2$.

(2) In the case of nonhomogeneous elliptic-cylinder, the magnitude of stresses is found to be low, whereas for homogeneous elliptic-cylinder it is high.

(3) The stresses are both tensile and compressive in different regions for different values of χ and ζ.

Manthena et al.: Thermal stress analysis in a functionally graded hollow elliptic

AAM: Intern. J., Vol 12, Issue 1 (June 2017)   631

(4) Special cases can also be studied by assigning suitable values to the material parameters in the equations of displacement and thermal stresses as well as by taking some different material for numerical computation.

REFERENCES

Abrinia K., Naee, H., Sadeghi, F. and Djavanroodi, F. (2008). New Analysis for the FGM Thick Cylinders Under Combined Pressure and Temperature Loading, American Journal of Applied Sciences, 5(7), 852-859.

Chen, W.Q., Ye, G.R. and Cai, J.B. (2001). A Uniformly Heated Functionally Graded Cylindrical Shell With Transverse Isotropy, Mechanics Research Communications, 283(5), 535-542.

Chen, W.Q, Ye, G.R. and Cai, J.B (2002). Thermoelastic Stresses in a uniformly heated functionally graded isotropic hollow cylinder, Journal of Zhejiang University SCIENCE, 3(1), 1-5.

Foroutan, M., Dastjerdi, R.M. and Bahreini, R.S. (2011). Static analysis of FGM cylinders by a mesh-free method, Steel and Composite Structures, 12(1), 1-11.

Ghannad, M. and Gharooni, H. (2012). Displacements and Stresses in Pressurized Thick FGM Cylinders with Varying Properties of Power Function Based on HSDT, Journal of Solid Mechanics, 4(3), 237-251.

Ghannad, M. and Gharooni, H. (2013). Displacements and Stresses in rotating FGM pressurized thick hollow cylinder with exponentially varying properties based on FSDT, Technical Journal of Engineering and Applied Sciences, 3(16), 1790-1799.

Hosseini, S.M. and Akhlaghi, M. (2009). Analytical solution in transient thermoelasticity of functionally graded thick hollow cylinders, Math. Methods Appl. Sci., 32(15), 2019-2034.

Khorshidvand, A.R. and Khalili, S.M.R. (2010). A new analytical solution for deformation and stresses in a Functionally Graded rotating cylinder subjected to thermal and mechanical loads, Proceedings of the 7th WSEAS international conference on heat and mass transfer, University of Cambridge, UK, 201-204.

Khorshidvand, A. R. and Javadi, M. (2012). Deformation and stress analysis in FG rotating hollow disk and cylinder subjected to thermal and mechanical loads, Applied Mechanics and Materials, 187, 68-73.

Kurşun, A., Kara, E., Çetin, E., Aksoy, Ş. and Kesimli, A. (2014). Mechanical and Thermal Stresses in Functionally Graded Cylinders, International Journal of Mechanical, Aerospace, Industrial, Mechatronic and Manufacturing Engineering, 8(2), 303-308.

Nejad, M.Z. and Rahimi, G.H. (2009). Deformations and stresses in rotating FGM pressurized thick hollow cylinder under thermal load, Scientific Research and Essay, 4(3),131-140.

Nejad, M.Z., Abedi, M., Lotfian, M.H. and Ghannad, M. (2012). An exact solution for stresses and displacements of pressurized FGM thick-walled spherical shells with exponential-varying properties, Journal of Mechanical Science and Technology, 26(12), 4081-4087.

Noda, N., Ootao, Y. and Tanigawa, Y. (2012). Transient thermoelastic analysis for a functionally graded circular disk with piecewise power law, Journal of theoretical and applied mechanics, 50(3), 831-839.

Ootao,Y. And Tanigawa, Y. (2005). Transient thermoelastic analysis for a functionally graded hollow cylinder, Journal of thermal stresses, 29(11),1031-1046.

Ravichandran, K.S. (1995). Thermal residual stresses in functionally graded material system, Materials Science Engineering A, 201(1-2), 269-276.

Takabi, B. (2016). Thermomechanical transient analysis of a thick-hollow FGM cylinder, Engineering Solid Mechanics, 4(1), 25-32.

Topal, S. and Gulgec, M. (2009). Thermal Stress Analysis of an FGM Cylinder under the Effect of Convection and Radially Varying Temperature Distribution, Materials Science Forum, 631-632, 23-28.

Tutuncu, N. (2007). Stresses in thick-walled FGM cylinders with exponentially-varying properties, Engineering Structures, 29(9),2032-2035.

Zimmerman, R.W. and Lutz, M.P. (1999). Thermal stresses and thermal expansion in a uniformly heated functionally graded cylinder, Journal of Thermal Stresses, 22(2), 177-188.